IEEE Access
Multidisciplinary | Rapid Review | Open Access Journal

Received 18 January 2023, accepted 1 February 2023, date of publication 6 February 2023, date of current version 9 February 2023.

Digital Object Identifier 10.1109/ACCESS.2023.3242692

RESEARCH ARTICLE

Broadband Supercontinuum Generation Using Dispersion Engineered As_2Se_3-GeAsSe-GeAsS Waveguide at 6μm

V. HITAISHI, (Member, IEEE), AND NANDAM ASHOK
Department of Physics, School of Advanced Sciences, VIT-AP University, Amaravati, Andhra Pradesh 522237, India
Corresponding author: Nandam Ashok (nandam.ashok@gmail.com)

This work was supported by VIT-AP University.

ABSTRACT This paper reports a theoretical study of supercontinuum generation with a novel dispersion-engineered reverse rib waveguide design using chalcogenide materials such as As_2Se_3 glass as a core, GeAsSe and GeAsS as cladding. This structure achieves an ultrawide bandwidth supercontinuum spectrum because of its high nonlinear property of core material and the low mode loss. The waveguide operates at 170fs laser sech pulses pumping at 6μm as a central wavelength. The proposed waveguide shows an ultra-wide spectrum of up to 16μm at 10kW peak power and up to 13μm broad spectrum at 5kW peak power. Results of spectral broadening for 2kW peak power are also discussed. The designed waveguide structure should be helpful in supercontinuum sources, bio-molecule sensing, and spectroscopy.

INDEX TERMS Chalcogenide glass, mode profile, sech pulse, stimulated Raman-scattering, supercontinuum generation, waveguide.

I. INTRODUCTION

Waveguides can be explained as a route map for the incident light pulses to travel through them. The characteristics of the waveguide and the interactions between incident light with the waveguide give an idea about the parameters like loss, dispersion, effective modes [1], [2], [3], [4], Nonlinear Coefficient (γ), nonlinear index (n_2), group velocity dispersion (GVD), Self-Phase Modulation (SPM) [5], Cross-phase Modulation (XPM) [6], soliton generation, Four-wave mixing (FWM) and stimulated Raman scattering (SRC) [7], [8], Two-photon absorption (TPA) and Multi-photon absorption (MPA) [9], [10]. Waveguides also respond uniquely in normal and anomalous dispersion regime.

Supercontinuum (SC) generation is a nonlinear optical process by pumping ultrashort (preferably femtosecond or picosecond) pulses into any optical waveguides. When light passes through the fiber or waveguide (around the core region) results in a spectral broadening by the interaction of the light source with the waveguide. SC generation has attracted much attention in recent years because of its wide range of applications in optical fiber communication [11], [12], coherence tomography [13], ultrafast amplifiers [14], frequency metrology, and many other fields. The supercontinuum spectrum generated in the infrared region is by the four-wave mixing between solitons and dispersive waves, self-frequency shift, and soliton fission [15], and the visible region of SC generation is by Cherenkov radiation [16], soliton trapping and cross-phase modulation [17].

Over the years, single and multi-mode fibers, tapered fibers, Photonic crystal fibers (PCF), and optical waveguides have been used to produce supercontinuum for different applications [18], [19]. The materials used to fabricate waveguides depend on the respective application. It is based on the range of wavelengths needed for the cause. Silicon glass (SiO_2) fibers were used when the range needed was visible and near-infrared region. Apart from this, heavy metal oxides were also used in this wavelength region. Fluoride glass fibers (ZBLAN, InF_3, ZrF) [20], [21] and liquid core fibers (CS_2, Ethanol) [22], [23] operate in the wavelength region of the visible, near-infrared, and near mid-infrared regions up to 4μm. Gas-filled hollow-core fibers (Ar, Xe,

The associate editor coordinating the review of this manuscript and approving it for publication was Md. Selim Habib.

Ne, Kr, H_2) [24], [25] can spread the spectrum from ultraviolet (0.2μm) to the near-mid infrared region up to 6μm. Moreover, silicon core and silicon-based fibers are used in the region between 0.4 and 8μm [26], [27]. Recently, chalcogenide glass fibers (S, Se, Te) have been utilized from near-infrared to mid-infrared regions, and studies are undergoing for mid-infrared to far-infrared regions [28], [29].

Low losses of chalcogen materials made these useful in all-optical switching, which is very important in the field of optical communication. There is a chance of TPA and MPA at lower wavelengths of the visible region, which helps broaden the spectrum. Using Degenerate four-wave mixing (DFWM), an experiment by Kanbara et al. [30] showed that an ultra-fast response time that is less than a picosecond can be achieved using chalcogenide materials.

The materials commonly considered to fabricate a waveguide or a PCF to generate SC generation are Silicon on Insulator (SOI) structures. David Duchesne et al. reported that a silicon waveguide with a core nonlinear index value of $n_2 = 5 \times 10^{-18}$ m^2/W does not demonstrate a wide range of spectral broadening [31]. However, it gave the idea to design waveguides to produce a broad spectrum. In the near-infrared and mid-infrared regions, Ahmad et al. modeled $Ge_{11.5}As_{24}Se_{64.5}$ chalcogenide waveguides with a broadband spectrum [32]. Step index fiber design modeled by Siwach P et al. used $Ge_{11.5}As_{24}Se_{64.5}$ to simulate SC generation has a high core nonlinear index value of $n_2 = 4.3 \times 10^{-18}$ m^2/W. They considered the central wavelength as 3.1μm, showing the dispersion of -11.36ps/(nm.km) using 10μm fiber pumped with 50fs pulse. It generates a spectrum from 2μm to 13μm pumping in a normal dispersion regime, which covers both near and part of mid-infrared regions [33]. Sharma R et al. modeled a 10μm long waveguide using GAP-Se and MgF_2 materials pumping with 45 to 135ps pulses at the center wavelength of 3100nm. This structure reports a chromatic dispersion of +21.63ps/(nm km) with a nonlinearity of 991(1/W.km), and the structure offers a supercontinuum spectrum ranging from 1.4 – 7.6μm [34].

Generation of supercontinuum by considering the optical waveguides with As_2Se_3 as a core material has a prominent role due to its higher refractive index over long wavelengths. Moreover, the linear and nonlinear properties of As_2Se_3 material show a good dispersion with the low loss with low latency interaction with the pulses. Yuan Wu demonstrated a single-mode PCF with As_2Se_3 material as a core of the fiber. The structure results in a spectral broadening from 2 to 10μm with a central wavelength of approximately 4μm [35]. Saini et al. reported mid-infrared SC generation with graded index As_2Se_3 PCF pumped at 4.1μm having 3.5kW peak power with 50fs pulses, which spans the supercontinuum from 2 μm to 15μm wavelength [36]. Yingying Wang et al. proposed a chalcogenide step-index fiber with As_2Se_3 as a core and As_2-As_2S as cladding pumped with 150fs pulses at 6.5μm central wavelength. The design achieved supercontinuum broadband from 2μm to 12.7μm [37]. Cherif et al. gave a numerical study on As_2Se_3-based chalcogenide PCF spanning 2 octaves using a central wavelength of 2.8μm [38]. Zhlutova et al., demonstrated a spectrally demonstrated flat SC generation in Silica-based dispersion decreasing fibers (DDF) with different core diameters and achieved a significant difference in the temporal and spectral transformation of radiation depending on the direction of wave propagation [39]. Kalashnikov et al., studied the Raman response in soft-glass PCFs in infrared supercontinuum generation to show that the Raman shift is double as high in the soft-glass as compared to fused silica [40]. Saini and Sinha gave a review about the Supercontinuum generations in Soft-glass PCFs in Mid-Infrared Region [41].

SC spectrum from any optical waveguides has been analyzed by numerically solving the Generalized Nonlinear Schrodinger Equation (GNLSE). This equation contains the interaction parameters of each phenomenon that occurs from linear and nonlinear effects. Several mathematical models and computational approaches are required to solve these equations and simulate high-energy pulse propagation in a waveguide. In this paper, the designing of waveguide and the propagation modes are obtained using COMSOL Multiphysics software. The Interaction picture method of Runge Kutta (RKIP4) in the frequency domain is used to calculate and produce SC generation.

Recently, Ashok et al. designed a reverse rib waveguide design for dispersion analysis. The structure shows a high negative dispersion, and the author discussed the fabrication tolerances [3]. The generation of the spectrum from waveguides depends upon the material properties, dimensions & design of waveguides, the central wavelength of input wave pumping, and power of the pulse, etc. In this paper, a reverse rib waveguide structure optical waveguide is discussed. The materials used to design and simulate the waveguide contain chalcogenide glasses like As_2Se_3 as a core covered with $Ge_{11.5}As_{24}Se_{64.5}$ around the core, and GeAsS covers the base and top. The proposed waveguide is optimized by changing the dimensions of the waveguide in order to obtain desired dispersion and to get a broad spectrum. At 6μm central wavelength, the designed waveguide has a loss of 1.9 dB/cm.

II. THEORY AND NUMERICAL ANALYSIS

In the present paper, a reverse rib-optical waveguide structure is proposed. The dimensions of the proposed waveguide are optimized for low loss at the pump wavelength. Optimization is done for the design for near-zero dispersion value around the central wavelength to achieve broad SC generation.

Chalcogenide glass materials have high Kerr nonlinearity. Its nonlinear index is roughly some hundred times that of silica at various operating wavelengths. That is why they are one of the most prominent in χ^3 (optical third-order nonlinear susceptibility) materials. The transmission range, ZDW, and refractive indices of the different materials are shown in Table 1 [28], [42].

The top and bottom strips of a waveguide are made by GeAsS with a height of 'f' (1.0μm) and a length of 'c'(16.0μm). The proposed waveguide's core is designed

TABLE 1. Materials with its optical properties.

Glass	Transmission Range (μm)	n_2/n_2 $(SiO_2)^3$	ZDW (μm)	Refractive Index
Silica	0.2-3.5	1.0	1.26	1.44
Tellurite glass	0.5-4.5	19	2.13	2.03
ZBLAN[1] glass	0.5-5.5	1.2	1.71	1.49
As_2S_3 ChG[2]	0.6-12	200	4.8	2.5
As_2Se_3 ChG	1.0-16	600	7.5	2.9
Te-based ChG	1.5-25	~1000	>7.5	~3.2

[1] ZBLAN, $ZrF_4 - BaF_2 - LaF_3 - AlF_3 - NaF$; [2] ChG, Chalcogenide Glass; [3] n_2, nonlinear refractive index

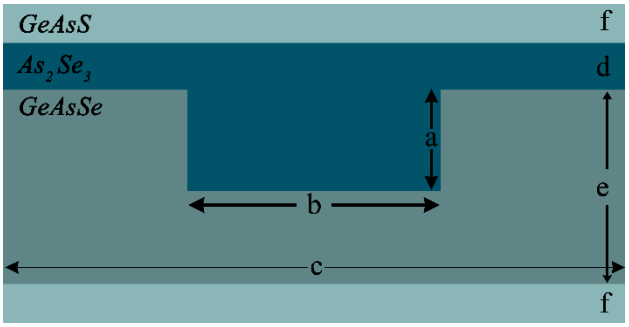

FIGURE 1. Optimized structure of proposed waveguide.

with a combination of a strip and a rectangle. The core strip height is 'd'(1.2μm). The rectangle core has a width of 'b' (6.5μm) and a height of 'a' (2.6μm) made with As_2Se_3 chalcogenide material. The length between the strip of core and the bottom strip of the waveguide is covered by GeAsSe material with the height 'e' (5.2μm). The designed waveguide is shown in Fig 1.

$$n(\lambda) = \sqrt{1 + \sum_{i=1}^{n} \frac{A_i \lambda^2}{\lambda^2 - B_i^2}} \tag{1}$$

The refractive indices of materials are plotted in Fig. 2 and calculated by utilizing the Sellmeier equation, shown in (1) (Here λ is in micrometer). The values of Sellmeier coefficients for $Ge_{11.5}As_{24}Se_{64.5}$, As_2Se_3, and GeAsS are given by Karim et al. [43], [44], and those are listed in Table 2: (Here B_i is in micrometer).

TABLE 2. Sellmeier coefficients of materials.

Materials	GeAsS	GeAsSe	As_2Se_3
A_1	4.18011	5.78525	4.994872
B_1	0.31679	0.28795	0.24164
A_2	0.35895	0.39705	0.120715
B_2	22.77018	30.39338	19
A_3			1.712369
B_3			0.48328

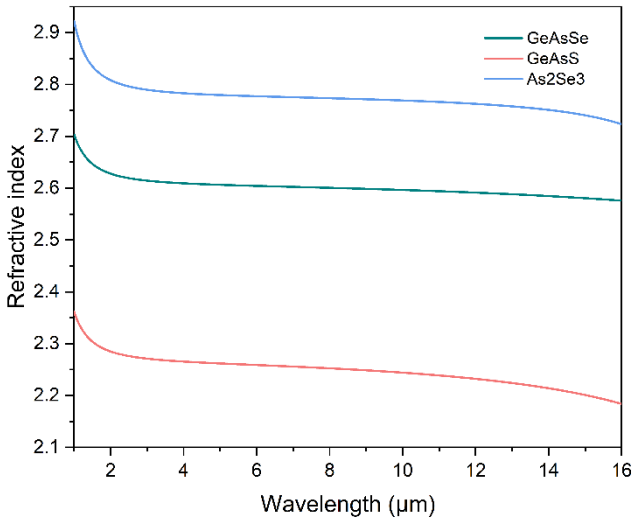

FIGURE 2. Effective indices of the materials as a function of wavelength.

The "Reverse- Rib" waveguide structure proposed here has some advantages in comparison with conventional designs. This structure confines the light modes more efficiently and also the fabrication of these types of designs is also easy [45]. Reverse ridge waveguide design can be fabricated in a crack-free manner. A groove should be created using GeAsSe substrate by reactive ion etching process (RIE), lower and upper slabs can be fabricated through Chemical Vapour Deposition (CVD) method. The core material As_2Se_3 can be filled in predefined trenches on the substrate using low-pressure chemical vapor deposition [3], [46], [47], [48].

Dispersion (D) can be calculated using two diverse ways, using n_{eff} or using $\beta(\omega)$. Here, the dispersion is solved numerically using (2) [1], [49], which results in values of dispersion for different wavelengths. From the dispersion graph, Zero Dispersion Wavelength (ZDW) is observed near 6μm, which helps in choosing the central wavelength to produce a supercontinuum.

$$D(\lambda) = -\frac{2\pi c}{\lambda^2}\frac{d^2\beta(\omega)}{d\omega^2}\,(or) - \frac{\lambda}{c}\frac{d^2 n_{eff}(\lambda)}{d\lambda^2} \tag{2}$$

By choosing appropriate waveguide parameters, the reverse waveguide structure shows −0.172ps/(nm.km) dispersion at the central wavelength of 6 μm.

$$\frac{\partial A}{\partial z} = -\frac{\alpha}{2}A - \left(\sum_{k\geq 2}\beta_k \frac{i^{k-1}}{k!}\frac{\partial^k}{\partial T^k}\right)A + i\gamma\left(1 + \frac{1}{\omega_o}\frac{\partial}{\partial T}\right) \times \left((1-f_R)|A|^2 + f_R\int_0^\infty h_R(\tau)\,|A(z,T-\tau)|^2\,d\tau\right)A \tag{3}$$

For the analysis of ultrashort pulses propagating through a waveguide, solving the Generalized nonlinear Schrodinger equation shown in (3) is necessary [1], [50]. Where A = A(z,t) is a time-varying input pulse at central frequency ω_o, α is a loss in the waveguide, and β_k's are the dispersion

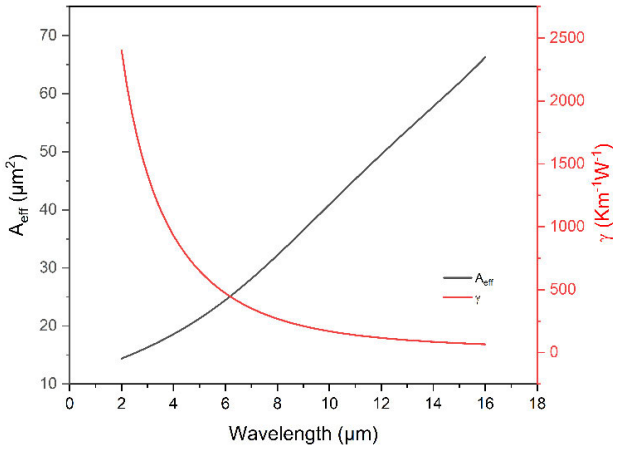

FIGURE 3. Effective area (A_{eff}) and nonlinear coefficient (γ) as a function of wavelength.

coefficients undergoing Taylor series expansion. β_k where ($k \leq 2$) are called Higher-order dispersion parameters (HODP), and it can be calculated by using (5) [49].

$$\beta_2 = -\frac{\lambda^2}{2\pi c} D \tag{4}$$

$$\beta_k = \frac{d\beta_{k-1}}{d\omega} \tag{5}$$

The second-order dispersion coefficient(β_2) is calculated by (4), and its higher-order dispersion coefficients are calculated by differentiating β_2 with respect to angular frequency(ω) (5). The nonlinear parameter (γ) is plotted as a function of wavelength in Fig. 3 and calculated using (6) [1], [24]:

$$\gamma = \frac{n_2 \omega_o}{c A_{eff}} (or) \frac{2\pi}{\lambda} \frac{n_2}{A_{eff}} \tag{6}$$

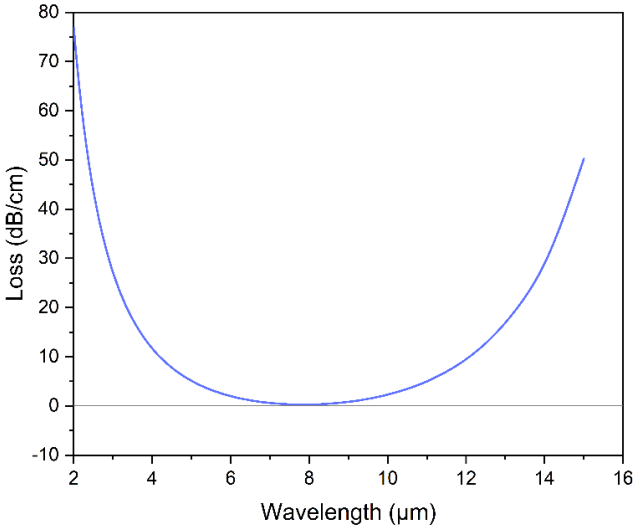

FIGURE 4. Waveguide loss.

where n_2 is the nonlinear index of core material (As_2Se_3) valued 1.1×10^{-17} m^2/W with $A_{eff} = 24.045$ μm^2, the nonlinear parameter value is 479.06 1/(W·km). Loss of waveguide is also considered and its variation with the wavelength is plotted in Fig. 4. Raman scattering is one of the significant phenomena during SC generation, which is also considered while solving GNLSE, where f_R is the Raman factor. At the center wavelength coefficients of Raman are $\tau_1 = 23$fs, $\tau_2 = 164.5$fs, and $f_R = 0.148$ [43].

$$R(t) = (1 - f_R)\,\delta(t) + f_R h_R(t) \tag{7}$$

$$h_R(t) = \frac{(\tau_1^2 + \tau_2^2)}{\tau_1 \tau_2^2} e^{-\left(\frac{t}{\tau_2}\right)} \sin\left(\frac{t}{\tau_1}\right) \tag{8}$$

The energy band gap of As_2Se_3 is significantly more than the combined energy of two and three incident photons, which is 0.413eV and 0.619eV. Due to an enormous difference between the energies. The effect of two and three-photon absorption can be neglected [9], [10].

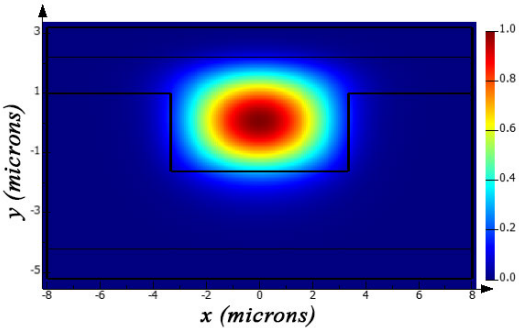

FIGURE 5. The Fundamental mode of the proposed waveguide at 6μm.

In the present structure with the optimized waveguide parameters, the modes of waveguides are calculated in order to measure the effective mode index and loss. Fundamental TE mode is considered in this paper, and the mode intensity profile is shown in Fig 5.

III. STRUCTURAL ANALYSIS & OPTIMIZATION

The proposed waveguide is optimized by various parameters for a better dispersion curve to generate broadband SC. The dispersion curve is calculated for the following optimized waveguide parameters, i.e., core height (a = 2.6 μm), core width (b = 6.5μm), top and bottom strip height (f = 1.0 μm), core strip height (d = 1.2 μm) and the waveguide width (c = 16 μm). Dispersion is plotted with wavelength for different values of core height (i.e., 2.2 μm, 2.4 μm, 2.6 μm, 2.8 μm, and 3.0 μm).

The tolerance study of core height is shown in Fig. 6. By increasing core height(a), the curve becomes slanted away from the horizontal axis, and by decreasing the value of 'a', the curve becomes flat towards the horizontal axis. For low values of core height, flat dispersion is achieved throughout some parts of the wavelength region. Such a flat dispersion curve is a good candidate for supercontinuum generation. Increasing the core height from 2.2 μm to 3.0 μm noticed that the dispersion values are increasing and the ZDW is moving towards the lower wavelength region.

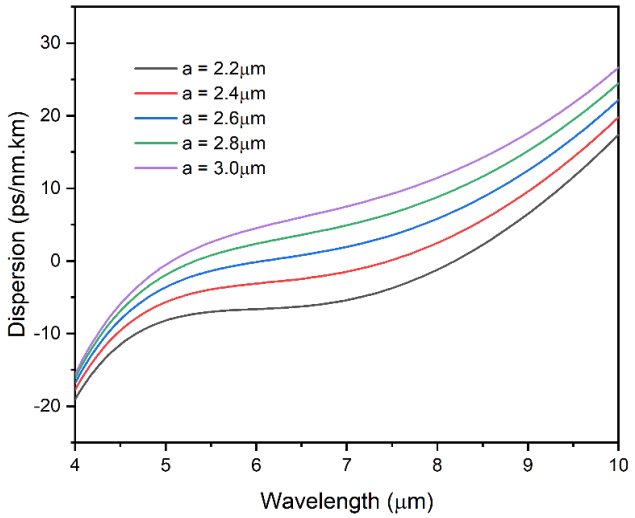

FIGURE 6. Dispersion graph using different core heights(a).

Fixing all the waveguide parameters except the core width, the effect of core width on the dispersion curve is analyzed. To adjust the central wavelength near to zero dispersion line, analysis of core width plays a crucial role in the proposed structure.

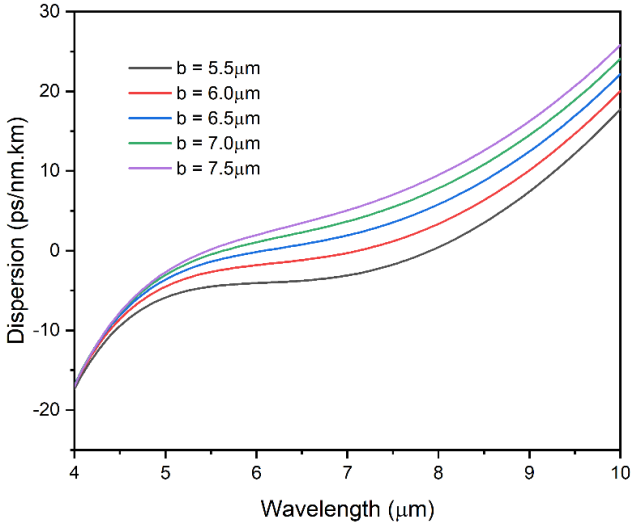

FIGURE 7. Dispersion graph for different core widths(b).

To investigate the core width effect, calculation of the dispersion curve for five different values of core width(b) are obtained and results are plotted in Fig 7. In the dispersion curve, as the core width increases, the line crossing zero dispersion shifts towards the lower end of the wavelength. As core width decreases, the curve is getting flattened in the middle of the wavelength range taken. From the figure, it is clear that for a core width of 5.5 μm, the curve shows zero dispersion at 7.9μm wavelength. As increasing core width to 6 μm, 6.5 μm, 7 μm, and 7.5 μm, the dispersion curve shows zero value near 7.1, 6, 5.65, and 5.45 μm wavelengths, respectively. From this result, it is evident that the effect of core width will help in choosing the central wavelength for SC generation.

Analysis of the effect of change in slab height(d) and the distance between core and cladding slab height(e) on the dispersion curve is considered. The obtained dispersion values are plotted in Fig 8(a) & Fig 8(b), respectively.

From Fig. 8(a), The trend of the dispersion curve remains almost the same and is noticeable. The impact of slab height changes is insignificant at the lower and upper end of the spectral range. However, there are some small widenings in a span of 5.5 to 8 μm wavelength range.

Changes in distance between the core slab and the cladding slab highly impacted the far side of the wavelength spectrum near, i.e., 9 to 10μm. Remarkable changes by tuning the value of 'e' shown in Fig 8(b) can be observed. This is because of the variation in the mode confinement of the input pulse. The lower index of the cladding material, with respect to the core material, pushes the mode towards the upper core when the lower slab is near the core region. If the lower slab is placed far from the core region, the propagation of the light spreads freely in core GeAsSe material.

The obtained results reveal that by choosing appropriate reverse rib-waveguide parameters, such as a strip height of 1.2μm, core width of 6.5 μm, a core height of 2.6μm, and distance between the core slab and the bottom strip of 5.2 μm. A low dispersion of -0.172ps/(nm.km) is observed at 6 μm wavelength and low loss at the same wavelength.

IV. SUPERCONTINUUM GENERATION

The fundamental Transverse Electric (TE) mode is considered for simulations. The sech pulse with a width of 12.5ps operating at 6μm wavelength is used to generate SC. The equation for the sech pulse is given in (9) [1]. The Full-width half maximum (FWHM) of the pulse is taken to be 170fs, and outputs are taken with different peak power of 2kW, 5kW, and 10kW.

$$A = \sqrt{P}\,\mathrm{sec}\,h\left(\frac{T}{t_o}\right) \tag{9}$$

Due to the high nonlinearity of As_2Se_3, the dispersion graph shows impressive results. The dispersion curve for the optimized waveguide parameters is plotted on Fig. 9. Values of HODP are calculated using the dispersion values with respect to frequency, and the accuracy of these values is important to solve GNLSE [49].

At central wavelength the dispersion lies in a normal dispersion regime, and the dispersion is found to be -0.172 ps/(nm.km). Loss at central wavelength is calculated, and it was found to be 1.9 dB/cm. SC generation needs a solver for the propagation of light through waveguides. Python code has been used to run the simulation based on a highly effective step-size implementation of the fourth order Runge-Kutta in the Interaction Picture (RK4IP) method [51], [52].

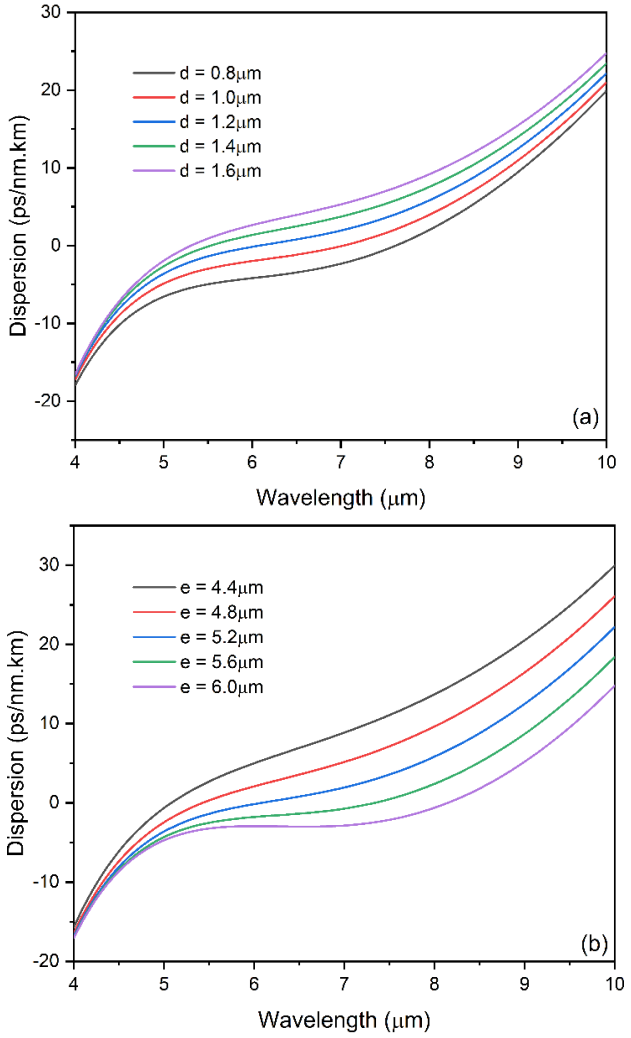

FIGURE 8. Dispersion curve for different (a) slab height(d), (b) length e.

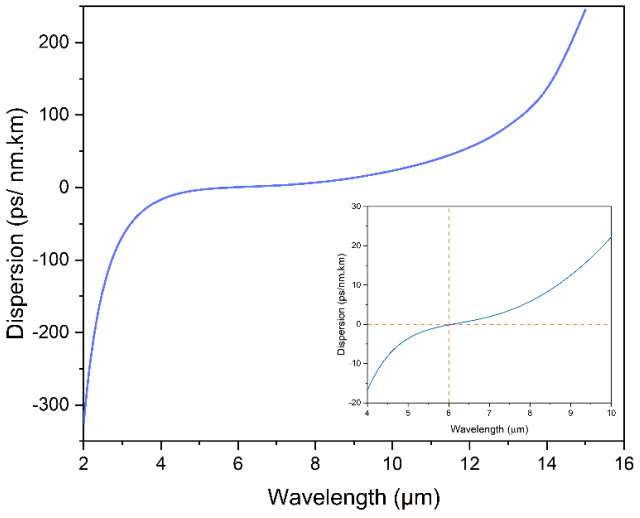

FIGURE 9. Dispersion curve for a proposed structure.

To generate broadband supercontinuum, 6μm wavelength pump is used near the zero dispersion wavelength value [43].

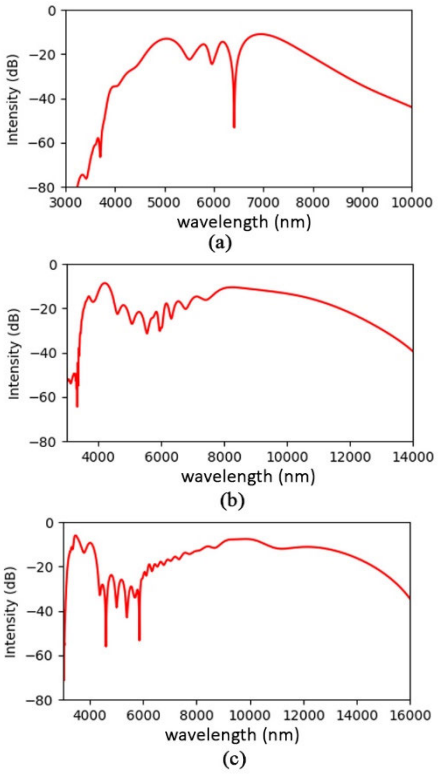

FIGURE 10. SC spectra for (a) 2kW, (b) 5kW, and (c) 10kW peak power.

Inputs in the present calculation are chosen to be 2kW, 5kW, and 10kW power with 170fs pulse duration (FWHM). Results from simulations of the supercontinuum spectra for the 2kW power spectral intensity is plotted in Fig 10(a) and its spectral evolution for same power is plotted in Fig. 11(a). It has been noticed that solition formations are less in this low-power input. However, the SPM and dispersions spam the spectra from 3.9 to 9.1 μm, hence covering a 5.2 μm wide spectrum.

Spectral analysis for 5kW input power is calculated for generating SC from the proposed waveguide, and supercontinuum results are plotted in Fig. 10(b). By choosing appropriate waveguide parameters, the reverse rib waveguide reports a wide spectrum broadening from 3.45 to 13.1 μm with 9.65 μm widening. Solitions formation can be seen around the central wavelength, and the solition fission occurs after input wave propagation towards half of the length of the waveguide. Dispersive wave radiations are near the 4 μm region of the spectra, and the higher end of spectra occurs with Raman dispersion and SPM. The spectral evolution for 5kW peak power is plotted in Fig. 11(b).

Next, analysis of the supercontinuum spectrum for 10kW peak power is undertaken. Fig. 10(c) reports the SC generation for a peak power of 10kW. Here SPM leads to a spectral broadening. Some of the incident lights are blue shifted towards the short wavelength side by fundamental solitons. Considering the suitable parameters with a change in power of 10kW leads to a spectral broadening of 12.9μm from 3.1 to 16μm. Soliton fission occurs around 5μm length

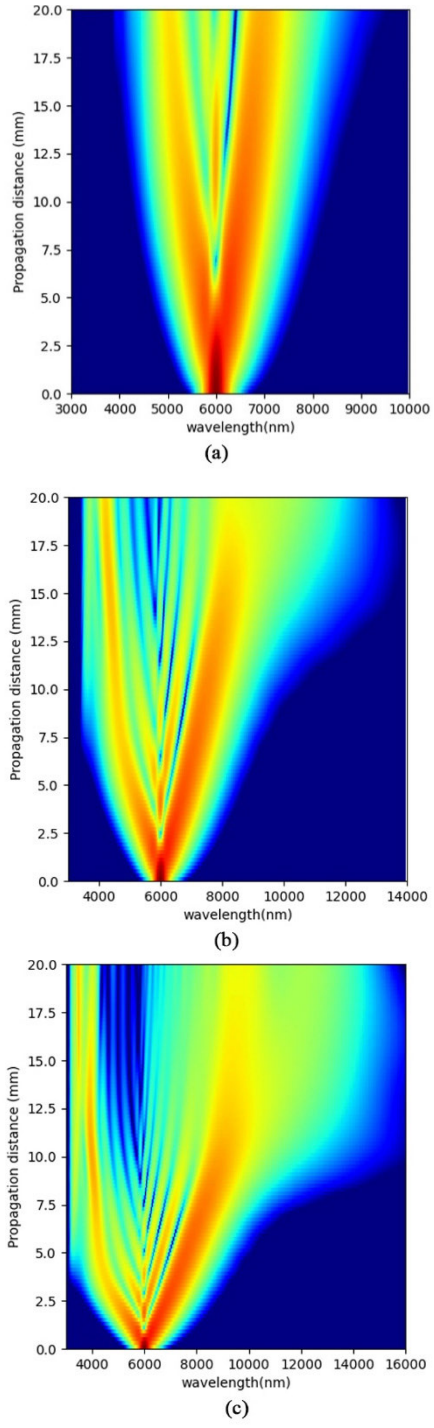

FIGURE 11. Spectral evolution of SC for (a) 2kW, (b) 5kW, and (c) 10kW peak power.

of the waveguide, and Blue shifted dispersive waves (DW) are noticed because of higher order dispersion before ZDW. The evolution of spectra for 10kW peak power is plotted in Fig. 11(c). From the above analysis, it is evident that the proposed structure achieves a broadband spectrum with the following designed parameters of a = 2.6μm, b = 6.5μm, c = 16.0μm, d = 1.2μm, e = 5.2μm and f = 1.0μm.

V. CONCLUSION

The waveguide proposed here is made by using GeAsS and $Ge_{11.5}As_{24}Se_{64.5}$ as cladding around the As_2Se_3 core and is modeled by taking into consideration of good dispersion curve around the center wavelength. The structure achieves a dispersion of -0.172 ps/(nm.km) at 6μm center wavelength. The reverse rib waveguide generates a 12.9 μm supercontinuum spectrum at the central wavelength of 6μm at 10kW peak power. We have also numerically simulated the supercontinuum for 5kW and 2kW peak power, and the structure results in 9.65 μm and 5.2 μm broad spectrums, respectively. The reported broadband spectrums are achieved with an input pulse of 170fs. The designed reverse rib waveguide can be used as a source for supercontinuum sources. These sources can be used to measure optical attenuation in photonic crystal fibers and to evaluate the laser and amplifiers [53].

ACKNOWLEDGMENT

The authors would like to thank the Vellore Institute of Technology, Vellore, for their assistance with the software.

REFERENCES

[1] J. M. Dudley and J. R. Taylor, *Supercontinuum Generation in Optical Fibers*. Cambridge, U.K.: Cambridge Univ. Press, 2010.
[2] N. Ashok, Y. L. Lee, and W. Shin, "Chalcogenide waveguide structure for dispersion in mid-infrared wavelength," *Jpn. J. Appl. Phys.*, vol. 56, no. 3, Feb. 2017, Art. no. 032501, doi: 10.7567/JJAP.56.032501.
[3] A. Nandam, M. Jung, Y. L. Lee, and W. Shin, "Reverse ridge silicon strip waveguide and silica slot waveguide structure for the dispersion at 1550 nm," *IEEE Photon. J.*, vol. 8, no. 6, pp. 1–9, Dec. 2016, doi: 10.1109/JPHOT.2016.2629083.
[4] V. Mann, N. Ashok, and V. Rastogi, "Coupled strip-slot waveguide design for dispersion compensation," *Opt. Quantum Electron.*, vol. 47, pp. 3161–3169, Apr. 2015, doi: 10.1007/s11082-015-0171-9.
[5] N. Tzoar and M. Jain, "Self-phase modulation in long-geometry optical waveguides," *Phys. Rev. A, Gen. Phys.*, vol. 23, no. 3, pp. 1266–1270, Mar. 1981, doi: 10.1103/PhysRevA.23.1266.
[6] V. G. Ta'eed, M. R. E. Lamont, D. J. Moss, B. J. Eggleton, D. Y. Choi, S. Madden, and B. L. Davis, "All optical wavelength conversion via cross phase modulation in chalcogenide glass rib waveguides," *Opt. Exp.*, vol. 14, no. 23, pp. 11242–11247, Oct. 2006, doi: 10.1364/OE.14.011242.
[7] H. Fukuda, K. Yamada, T. Shoji, M. Takahashi, T. Tsuchizawa, T. Watanabe, J. Takahashi, and S. Itabashi, "Four-wave mixing in silicon wire waveguides," *Opt. Exp.*, vol. 13, no. 12, pp. 4629–4637, Jun. 2005, doi: 10.1364/OPEX.13.004629.
[8] S. Signorini, M. Mancinelli, M. Bernard, M. Bernard, M. Ghulinyan, G. Pucker, and L. Pavesi, "Intermodal four-wave mixing in silicon waveguides," *Photon. Res.*, vol. 6, no. 8, pp. 805–814, Jul. 2018, doi: 10.1364/PRJ.6.000805.
[9] M. Rumi and J. W. Perry, "Two-photon absorption: An overview of measurements and principles," *Adv. Opt. Photon.*, vol. 2, no. 4, pp. 451–518, Dec. 2010, doi: 10.1364/AOP.2.000451.
[10] E. W. Van Stryland, M. A. Woodall, H. Vanherzeele, and M. J. Soileau, "Energy band-gap dependence of two-photon absorption," *Opt. Lett.*, vol. 10, no. 10, pp. 490–492, Oct. 1985, doi: 10.1364/OL.10.000490.
[11] K. Worhoff, P. V. Lambeck, and A. Driessen, "Design, tolerance analysis, and fabrication of silicon oxynitride based planar optical waveguides for communication devices," *J. Lightw. Technol.*, vol. 17, no. 8, pp. 1401–1407, 1999.
[12] H. Yamada, T. Chu, S. Ishida, and Y. Arakawa, "Optical directional coupler based on Si-wire waveguides," *IEEE Photon. Technol. Lett.*, vol. 17, no. 3, pp. 585–587, Mar. 2005, doi: 10.1109/LPT.2004.840926.
[13] D. Culemann, A. Knuettel, and E. Voges, "Integrated optical sensor in glass for optical coherence tomography (OCT)," *IEEE J. Sel. Topics Quantum Electron.*, vol. 6, no. 5, pp. 730–734, Sep. 2000, doi: 10.1109/2944.892611.

[14] J. Mørk and A. Mecozzi, "Theory of the ultrafast optical response of active semiconductor waveguides," *J. Opt. Soc. Amer. B, Opt. Phys.*, vol. 13, no. 8, pp. 1803–1816, Aug. 1996, doi: 10.1364/JOSAB.13.001803.

[15] A. V. Husakou and J. Herrmann, "Supercontinuum generation, four-wave mixing, and fission of higher-order solitons in photonic-crystal fibers," *J. Opt. Soc. Amer. B, Opt. Phys.*, vol. 19, no. 9, pp. 2171–2182, Sep. 2022, doi: 10.1364/JOSAB.19.002171.

[16] H. Tu and S. A. Boppart, "Optical frequency up-conversion by supercontinuum-free widely-tunable fiber-optic Cherenkov radiation," *Opt. Exp.*, vol. 17, no. 12, pp. 987–9858, May 2009, doi: 10.1364/OE.17.009858.

[17] S. Hill, C. E. Kuklewicz, U. Leonhardt, and F. König, "Evolution of light trapped by a soliton in a microstructured fiber," *Opt. Exp.*, vol. 17, no. 16, pp. 13588–13601, Jul. 2009, doi: 10.1364/OE.17.013588.

[18] S. Coen, A. H. L. Chau, R. Leonhardt, J. D. Harvey, J. C. Knight, W. J. Wadsworth, and P. S. J. Russell, "Supercontinuum generation by stimulated Raman scattering and parametric four-wave mixing in photonic crystal fibers," *J. Opt. Soc. Amer. B, Opt. Phys.*, vol. 19, no. 4, pp. 753–764, 2002, doi: 10.1364/JOSAB.19.000753.

[19] I. Cerutti, N. Andriolli, and P. Velha, "Engineering of closely packed silicon-on-isolator waveguide arrays for mode division multiplexing applications," *J. Opt. Soc. Amer. B, Opt. Phys.*, vol. 34, no. 2, pp. 497–506, Jan. 2017, doi: 10.1364/JOSAB.34.000497.

[20] L. Yang, B. Yan, R. Zhao, D. Wu, T. Xu, P. Yang, Q. Nie, and S. Dai, "Ultra-low fusion splicing loss between silica and ZBLAN fiber for all-fiber structured high-power mid-infrared supercontinuum generation," *Infr. Phys. Technol.*, vol. 113, Mar. 2021, Art. no. 103576, doi: 10.1016/j.infrared.2020.103576.

[21] J. Swiderski, "Recent development of mid-infrared supercontinuum generation in fluoroindate glass fibers," *Appl. Sci.*, vol. 12, no. 10, p. 4927, May 2022, doi: 10.3390/app12104927.

[22] R. Zhang, J. Teipel, and H. Giessen, "Theoretical design of a liquid-core photonic crystal fiber for supercontinuum generation," *Opt. Exp.*, vol. 14, pp. 6800–6812, Jul. 2006, doi: 10.1364/OE.14.006800.

[23] R. Scheibinger, N. M. Lupken, M. Chemnitz, K. Schaarschmidt, J. Kobelke, C. Fallnich, and M. A. Schmidt, "Higher-order mode supercontinuum generation in dispersion-engineered liquid-core fibers," *Sci. Rep.*, vol. 11, no. 1, p. 5270, Mar. 2021, doi: 10.1038/s41598-021-84397-1.

[24] A. I. Adamu, M. S. Habib, C. R. Petersen, J. E. A. Lopez, B. Zhou, A. Schulzgen, M. Bache, R. Amezcua-Correa, O. Bang, and C. Markos, "Deep-UV to mid-IR supercontinuum generation driven by mid-IR ultrashort pulses in a gas-filled hollow-core fiber," *Sci. Rep.*, vol. 9, no. 1, pp. 1–9, Mar. 2019, doi: 10.1038/s41598-019-39302-2.

[25] M. F. Saleh and F. Biancalana, "Ultra-broadband supercontinuum generation in gas-filled photonic-crystal fibers: The epsilon-near-zero regime," *Opt. Lett.*, vol. 46, no. 8, pp. 1959–1962, Apr. 2021, doi: 10.1364/OL.421649.

[26] H. L. Van, V. T. Hoang, Q. H. Dinh, H. T. Nguyen, N. V. T. Minh, M. Klimczak, R. Buczynski, and R. Kasztelanic, "Silica-based photonic crystal fiber infiltrated with 1,2-dibromoethane for supercontinuum generation," *Appl. Opt.*, vol. 60, no. 24, pp. 7268–7278, Aug. 2021, doi: 10.1364/AO.430843.

[27] V. A. Kamynin, A. S. Kurkov, and V. M. Mashinsky, "Supercontinuum generation up to 2.7 μm in the germanate-glass-core and silica-glass-cladding fiber," *Laser Phys. Lett.*, vol. 9, no. 3, pp. 219–222, Jan. 2012, doi: 10.1002/lapl.201110115.

[28] S. Dai, Y. Wang, X. Peng, P. Zhang, X. Wang, and Y. Xu, "A review of mid-infrared supercontinuum generation in chalcogenide glass fibers," *Appl. Sci.*, vol. 8, no. 5, p. 707, May 2018, doi: 10.3390/app8050707.

[29] H. T. Tong, A. Koumura, A. Nakatani, H. P. T. Nguyen, M. Matsumoto, G. Sakai, T. Suzuki, and Y. Ohishi, "Chalcogenide all-solid hybrid microstructured optical fiber with polarization maintaining properties and its mid-infrared supercontinuum generation," *Opt. Exp.*, vol. 30, no. 14, pp. 25433–25449, Jun. 2022, doi: 10.1364/OE.459745.

[30] H. Kanbara, S. Fujiwara, K. Tanaka, H. Nasu, and K. Hirao, "Third-order nonlinear optical properties of chalcogenide glasses," *Appl. Phys. Lett.*, vol. 70, no. 8, pp. 925–927, Feb. 1997, doi: 10.1063/1.118443.

[31] D. Duchesne, M. Peccianti, M. R. E. Lamont, M. Ferrera, L. Razzari, F. Legare, R. Morandotti, S. Chu, B. E. Little, and D. J. Moss, "Supercontinuum generation in a high index doped silica glass spiral waveguide," *Opt. Exp.*, vol. 18, no. 2, pp. 923–930, Jan. 2010, doi: 10.1364/OE.18.000923.

[32] H. Ahmad, M. R. Karim, and B. M. A. Rahman, "Modeling of dispersion engineered chalcogenide rib waveguide for ultraflat mid-infrared supercontinuum generation in all-normal dispersion regime," *Appl. Phys. B*, vol. 124, no. 3, pp. 1–10, Feb. 2018, doi: 10.1007/s00340-018-6914-0.

[33] P. Siwach, A. Kumar, and T. S. Saini, "Broadband supercontinuum generation spanning 1.5–13 μm in $Ge_{11.5}As_{24}Se_{64.5}$ based chalcogenide glass step index optical fiber," *Optik*, vol. 156, pp. 564–570, Mar. 2018, doi: 10.1016/j.ijleo.2017.11.199.

[34] R. Sharma, S. Kaur, P. Chauhan, and A. Kumar, "Computational design & analysis of $GeSe_2$-As_2Se_3-PbSe based rib waveguide for mid-infrared supercontinuum generation," *Optik*, vol. 220, Oct. 2020, Art. no. 165032, doi: 10.1016/j.ijleo.2020.165032.

[35] W. Yuan, "2–10 μm mid-infrared supercontinuum generation in As_2Se_3 photonic crystal fiber," *Laser Phys. Lett.*, vol. 10, no. 9, Aug. 2013, Art. no. 095107, doi: 10.1088/1612-2011/10/9/095107.

[36] T. S. Saini, A. Kumar, and R. K. Sinha, "Broadband mid-infrared supercontinuum spectra spanning 2–15 μm using As_2Se_3 chalcogenide glass triangular-core graded-index photonic crystal fiber," *J. Lightw. Technol.*, vol. 33, no. 18, pp. 3914–3920, Sep. 15, 2015.

[37] Y. Wang, S. Dai, X. Han, P. Zhang, Y. Liu, X. Wang, and S. Sun, "Broadband mid-infrared supercontinuum generation in novel As_2Se_3-As_2Se_2S step-index fibers," *Opt. Commun.*, vol. 410, pp. 410–415. Mar. 2018, doi: 10.1016/j.optcom.2017.10.056.

[38] R. Cherif, A. B. Salem, M. Zghal, P. Besnard, T. Chartier, L. Brilland, and J. Troles, "Highly nonlinear As_2Se_3-based chalcogenide photonic crystal fiber for midinfrared supercontinuum generation," *Opt. Eng.*, vol. 49, no. 9, Sep. 2010, Art. no. 095002, doi: 10.1117/1.3488042.

[39] I. V. Zhluktova, V. A. Kamynin, D. A. Korobko, A. S. Abramov, A. A. Fotiadi, A. A. Sysoliatin, and V. B. Tsvetkov, "Broadband supercontinuum generation in dispersion decreasing fibers in the spectral range 900–2400 nm," *Photonics*, vol. 9, no. 10, p. 773, Oct. 2022, doi: 10.3390/photonics9100773.

[40] V. L. Kalashnikov, E. Sorokin, and I. T. Sorokina, "Raman effects in the infrared supercontinuum generation in soft-glass PCFs," *Appl. Phys. B, Lasers Opt.*, vol. 87, no. 1, pp. 37–44, Mar. 2007, doi: 10.1007/s00340-006-2545-y.

[41] T. S. Saini and R. K. Sinha, "Mid-infrared supercontinuum generation in soft-glass specialty optical fibers: A review," *Prog. Quantum Electron.*, vol. 78, Aug. 2021, Art. no. 100342, doi: 10.1016/j.pquantelec.2021.100342.

[42] G. Tao, H. E. Heidepriem, A. M. Stolyarov, S. Danto, J. V. Badding, Y. Fink, J. Ballato, and A. F. Abouraddy, "Infrared fibers," *Adv. Opt. Photon.*, vol. 7, no. 2, pp. 379–458, Jun. 2015, doi: 10.1364/AOP.7.000379.

[43] M. R. Karim, H. Ahmad, S. Ghosh, and B. M. A. Rahman, "Design of dispersion-engineered As_2Se_3 channel waveguide for mid-infrared region supercontinuum generation," *J. Appl. Phys.*, vol. 123, no. 21, Jun. 2018, Art. no. 213101, doi: 10.1063/1.5033494.

[44] M. R. Karim, H. Ahmad, and B. M. A. Rahman, "Design and modeling of dispersion-engineered all-chalcogenide triangular-core fiber for mid-infrared-region supercontinuum generation," *J. Opt. Soc. Amer. B, Opt. Phys.*, vol. 35, no. 2, pp. 266–275, Jan. 2018, doi: 10.1364/JOSAB.35.000266.

[45] M. Yako, C. Park, D. Ahn, Y. Ishikawa, and K. Wada, "Low threshold light emission from reverse-rib n^+ Ge cavity made by P diffusion," *ECS Trans.*, vol. 75, no. 8, pp. 193–198, Aug. 2016, doi: 10.1149/07508.0193ecst.

[46] Z. Hui, L. Zhang, and W. Zhang, "CMOS compatible on-chip telecomband to mid-infrared supercontinuum generation in dispersion-engineered reverse strip/slot hybrid Si_3N_4 waveguide," *J. Modern Opt.*, vol. 65, no. 1, pp. 53–63, Jan. 2018, doi: 10.1080/09500340.2017.1376718.

[47] J. P. Epping, M. Hoekman, R. Mateman, A. Leinse, R. G. Heideman, A. V. Rees, P. J. M. Van Der Slot, C. J. Lee, and K.-J. Boller, "High confinement, high yield Si_3N_4 waveguides for nonlinear optical applications," *Opt. Exp.*, vol. 23, no. 2, pp. 642–648, Jan. 2015, doi: 10.1364/OE.23.000642.

[48] Y. Zhai, C. Yuan, R. Qi, W. Zhang, and Y. Huang, "Reverse ridge/slot chalcogenide glass waveguide with ultrabroadband flat and low dispersion," *IEEE Photon. J.*, vol. 7, no. 5, pp. 1–9, Oct. 2015, doi: 10.1109/JPHOT.2015.2456062.

[49] A. Martínez-Rios, B. Ilan, I. Torres-Gómez, D. Monzon-Hernandez, and D. E. Ceballos-Herrera, "Calculation of higher order dispersion coefficients in photonic crystal fibers," in *Proc. SPIE*, vol. 8011, pp. 106–115, Oct. 2011, doi: 10.1117/12.901625.

[50] Y. Cao, B.-U. Sohn, H. Gao, P. Xing, G. F. R. Chen, D. K. T. Ng, and D. T. H. Tan, "Supercontinuum generation in a nonlinear ultra-silicon-rich nitride waveguide," *Sci. Rep.*, vol. 12, no. 1, p. 9487, Jun. 2022, doi: 10.1038/s41598-022-13734-9.
[51] J. Hult, "A fourth-order Runge–Kutta in the interaction picture method for simulating supercontinuum generation in optical fibers," *J. Lightw. Technol.*, vol. 25, no. 12, pp. 3770–3775, Dec. 2007.
[52] J. C. H. Garcia, J. M. E. Ayala, O. Pottiez, J. P. L. Cruz, J. D. F. Razo, J. R. M. Angulo, C. M. C. Delgado, D. J. Vazquez, J. M. S. Hernandez, and R. R. Laguna, "Application of the RK4IP Method for the numerical study of noise-like pulses in supercontinuum generation," in *Proc. Electromagn. Res. Symp.*, 2018, pp. 805–809, doi: 10.23919/PIERS.2018.8597917.
[53] N. Savage, "Supercontinuum sources," *Nature Photon.*, vol. 3, no. 2, pp. 114–115, Feb. 2009, doi: 10.1038/nphoton.2008.286.

V. HITAISHI (Member, IEEE) was born in Karnataka, India, in January 1998. He received the Bachelor of Science degree in physics, chemistry, and mathematics from the Dayananda Sagar College of Arts, Science and Commerce, Bengaluru, Karnataka, in 2018, and the Master of Science degree in physics from the JSS College of Arts, Commerce and Science, Mysore, Karnataka, in 2020. He is currently pursuing the Ph.D. degree in nonlinear optics (waveguides for various applications) with VIT-AP University.

NANDAM ASHOK received the B.Sc. degree in mathematics, physics, and chemistry from the SRR & CVR Govt. Degree College, Vijayawada, Andhra Pradesh, India, the M.Sc. degree in physics from the ANR College, Gudivada, Andhra Pradesh, and the Doctoral (Ph.D.) degree from the IIT Roorkee, India, in April 2014, under the supervision of Prof. Vipul Rastogi.

From November 2014 to September 2015, he worked as a Postdoctoral Researcher at the Center for Photon Information Processing, Gwangju Institute of Science and Technology, South Korea. He worked as a Postdoctoral Researcher at the Advanced Photonics Research Institute, Gwangju Institute of Science and Technology, from October 2015 to September 2018. Currently, he is working as an Assistant Professor with VIT-AP University. He has published some articles, such as "Dual core leaky waveguide based filters for erbium-doped waveguide amplifier" (*Fiber and Integrated Optics*), "Spiral photonic crystal fiber structure for supporting orbital angular momentum modes" (*Optik*), and "Reverse ridge silicon strip waveguide and silica slot waveguide structure for the dispersion at 1550 nm" (IEEE Photonics Journal). His research interests include photonic crystal fiber sensors, OAM modes in photonic crystal fibers, plasmonic waveguides, high-power fiber lasers, quantum memory in fibers and waveguides, quantum integrated optics, long period waveguide gratings as a filter and sensor, and design of plasmonic solar cells.